Supporting Information

Reconstruction of Nitrogen-containing Covalent Organic Framework Coordinated Ir Single-atom Electrocatalysts for High-performance Lithium-rich Oxygen Battery Cathodes

Babar Shahzad[abcd], Yihui Li[abcd], Dong Xinfang[abcd], Yangjian Ding[abcd], Zewen Xu[abcd], Muhammad Kashif Zaman[e], Rana Muhammad Irfan[abc], Cheng Huang*[abcd]*

[a] College of Energy, Soochow Institute for Energy and Materials InnovationS (SEIMIS), College of Energy, Soochow University, Suzhou 215006, P.R. China.

[b] Key Laboratory of Advanced Carbon Materials and Wearable Energy Technologies of Jiangsu Province, Soochow University, Suzhou 215006, P.R. China.

[c] Suzhou Institute of Electronic Functional Materials Technology, Suzhou 215006, P.R. China.

[d] Key Laboratory of Core Technology of High Specific Energy Battery and Key Materials for Petroleum and Chemical Industry, Soochow University, Suzhou 215006, P.R. China.

[e] Department of Pharmacy, Shanghai Jiao Tong University, Shanghai 200240, China.

Corresponding Authors:
*E-mail: irfan45@mail.ustc.edu.cn. chengh@suda.edu.cn Phone: +8613166133072

PHYSICAL CHARACTERIZATIONS

The morphology, composition, and structure of prepared samples were characterized by scanning electron microscope (SEM, Hitachi SU8010, 10 kV), Transmission electron microscope (TEM, FEI Themis Z, Thermo Fisher Scientific 60-300 keV), spherical aberration (Cs) corrected TEM (FEI Titan Themis Cubed G2 300). The crystal structures of all the samples were characterized using X-ray diffraction (XRD) at $0.02°s^{-1}$ with an X-ray diffractometer (D8 Advance Instrument; Cu Kα radiation; operated at 40 kV, 45 mA, λ = 0.15418 nm). The Raman spectra were obtained using a Raman spectrometer with a backscattering geometry (λ = 633 nm; HR Evolution, HORIBA JOBIN-YVON). The binding environment of all elements in the produced samples was investigated using an X-ray photoelectron spectrometer (XPS, Thermos Fisher ESCALAB 250xi) equipped with a monochromatized Al Kα (1486.6 eV) source that was adjusted for background using the Shirley method. 'Thermo Avantage' software was used to process the XPS data. The Brunauer-Emmett-Teller (BET, Micromeritics, Tristar II 3020) was used to calculate the surface areas of all the samples. *L3*-edge analysis was performed with Si(111) crystal monochromators at the BL14W1 beamlines at the Shanghai Synchrotron Radiation Facility (SSRF) (Shanghai, China). Before the analysis at the beamline, samples were pressed into thin sheets with 1 cm in diameter and sealed using Kapton tape film. The XAFS spectra were recorded at room temperature using a 4-channel Silicon Drift Detector (SDD) Bruker 5040. Ir *L3*-edge extended X-ray absorption fine structure (EXAFS) spectra were recorded in transmission mode. Negligible changes in the line-shape and peak position of Ir *L3*-edge XANES spectra were observed between two scans taken for a specific sample. The XAFS spectra of these standard samples (Ir, IrO_2) were recorded in transmission mode. The spectra were processed and analyzed by the software codes Athena and Artemis. The XAFS results were fitted via the IFEFFIT

software. Thermogravimetric analysis (TGA) was carried out on a thermogravimetric analyzer (TG/DTA7300, SII NanoTechnology) with 2–3 mg of sample in a SiO_2 pan at a heating rate of 10°C /min. Ir content in as-synthesized Ir/N-PAQR SAC was checked by ICP-OES, PerkinElmer OPTIMA 8000DV, respectively.

ELECTROCHEMICAL MEASUREMENTS

The working electrode was fabricated by mixing 80 wt% active materials (Ir/COF SA/NP), 10 wt% carbon black as a conductive additive, and 10 wt% polyvinylidene fluoride (PVDF, Du Pont-Mitsui Fluor chemicals Co, Ltd) as a binder in N-methyl pyrrolidine (NMP, NMP, Sigma Aldrich, 99%). The obtained slurry was homogeneously coated on an aluminum (Al) foil current collector by a scraper (0.1mm height). The coated Al foil was dried at 80°C for 12 h, and the final electrode plates (11mm) were punched out. The total mass loading for each cathode plate was 2.0-2.2mg cm^{-2}. Coin-type (CR2032) cells were assembled in an argon-filled glove box containing less than 0.1 ppm of oxygen and water contents, respectively. A solution of 1.0 M LiPF6 in ethylene carbonate/diethyl carbonate (EC: DEC = 1:1 v/v) was used as electrolyte. Lithium foil and polypropylene and polyethylene film were used as counter electrodes and separators, respectively. Cyclic voltammetry (CV) measurements were carried out on the (CHI660E electrochemical analyzer) over the range of 1.5- 4 V at a scan rate of 0.1 mV s^{-1}. Electrochemical impedance spectroscopy (EIS) measurements were performed using (CHI660E electrochemical workstation). The impedance spectra were obtained by applying an AC voltage of 10 mV over the frequency range from 0.1- 100 kHz at room temperature. The charge-discharge profiles, cycling, and rate performance were tested over the range of 1.5- 4 V using a LANDTE CT2001A battery test system. The current density was normalized at 897 mAh g^{-1} based on the active material (Li_2O), which is equal to a 1.0 C current rate.
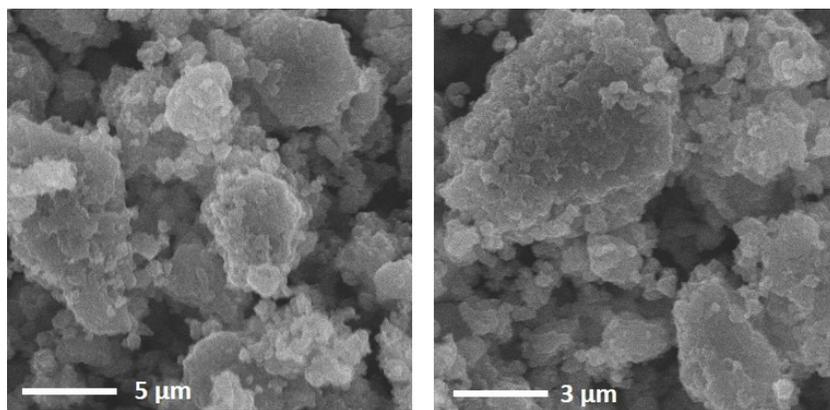
Figure S-1. SEM images of COF
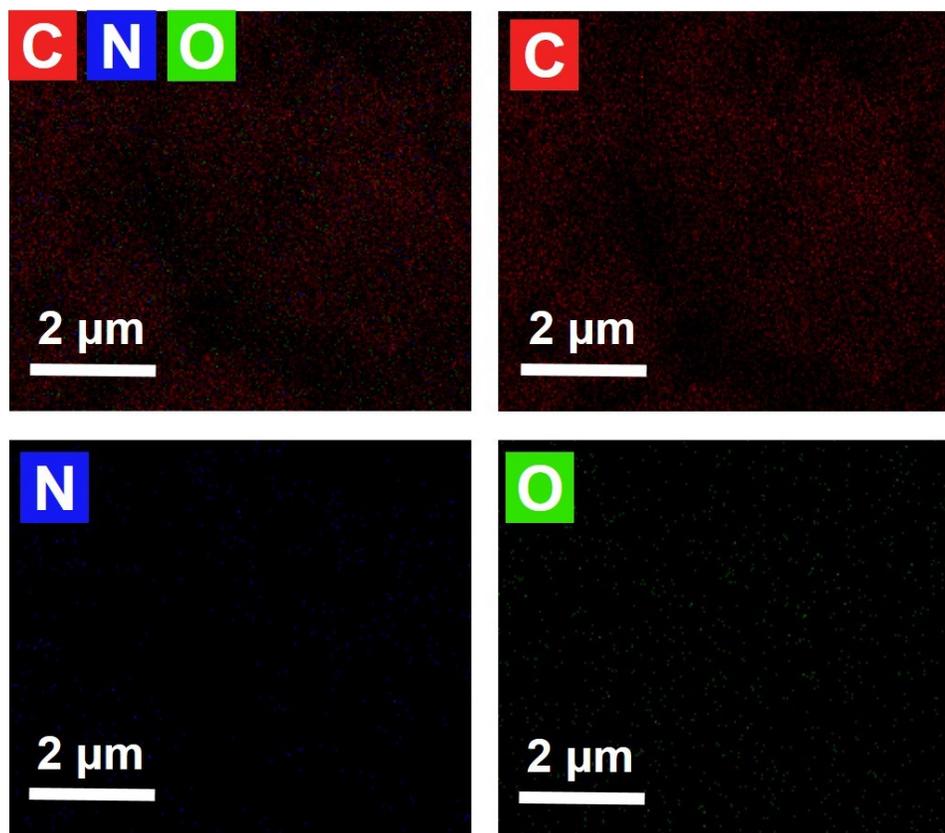
Figure S-2. EDS mapping images of COF
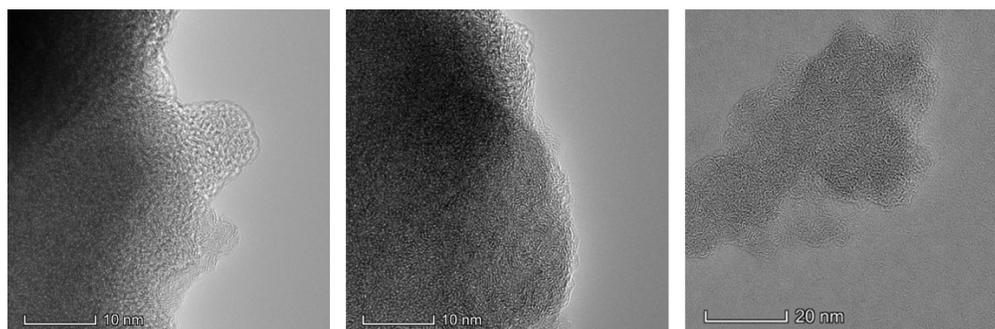
Figure S-3. HR-TEM images of COF
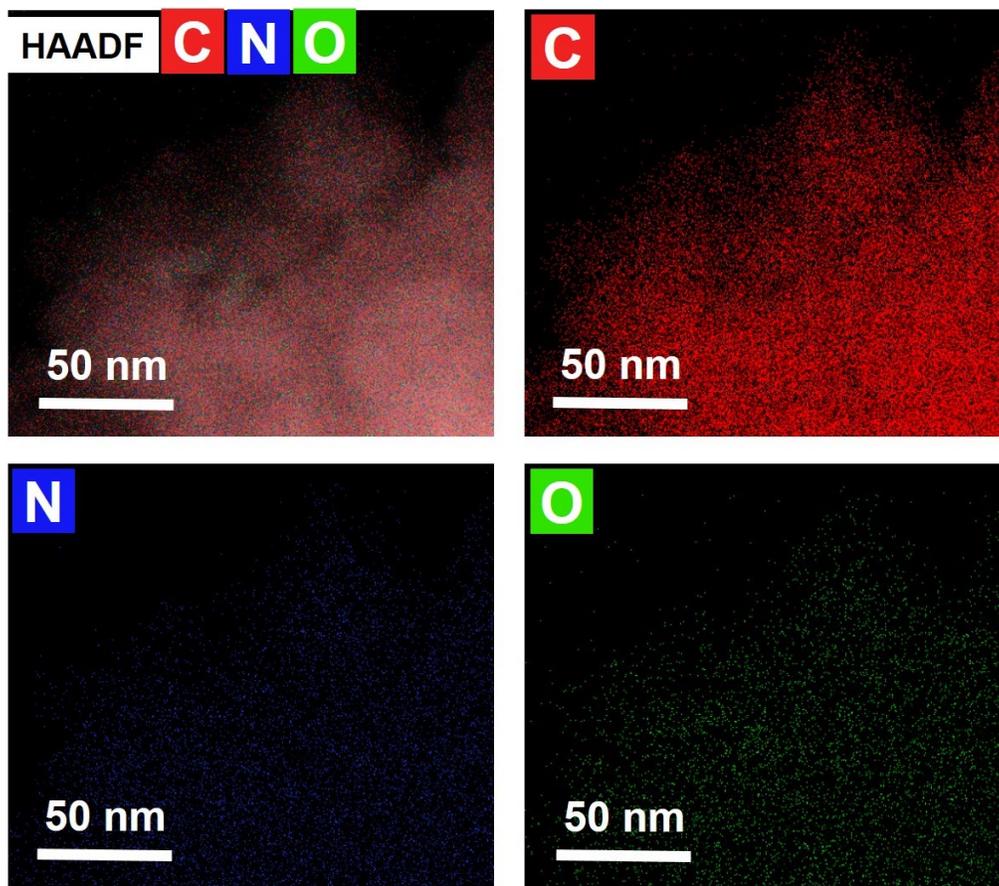
Figure S-4. STEM EDS mapping images of COF
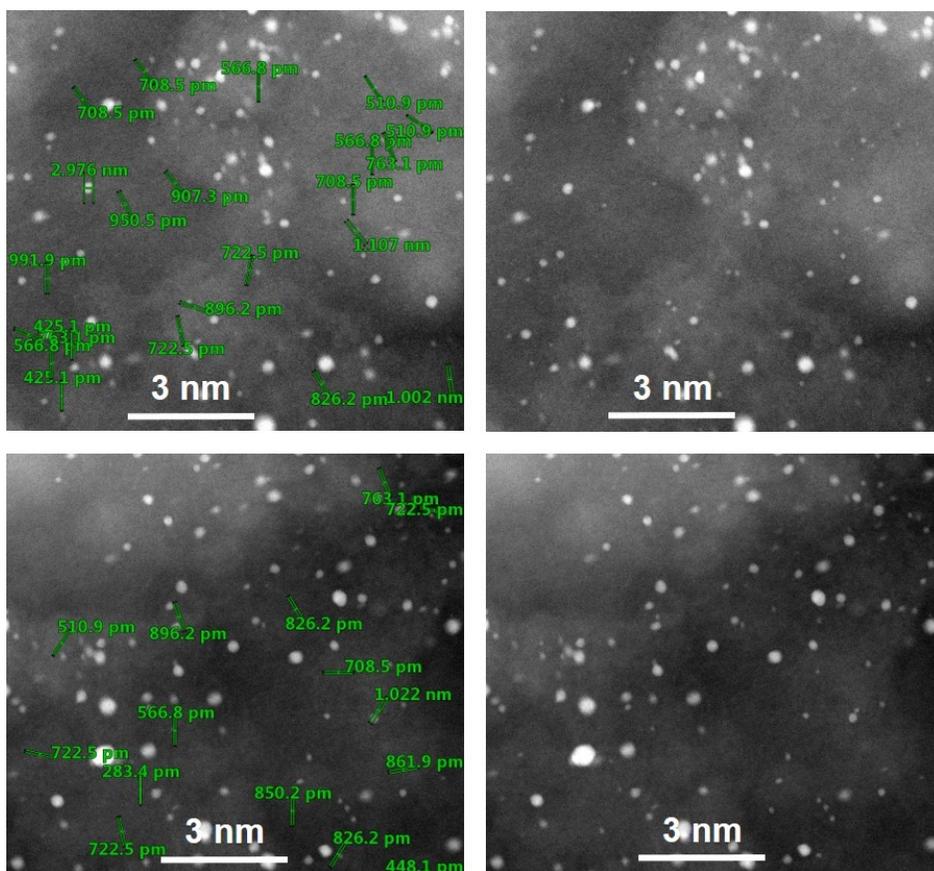
Figure S-5. HAADF-STEM images Ir/COF SA/NP
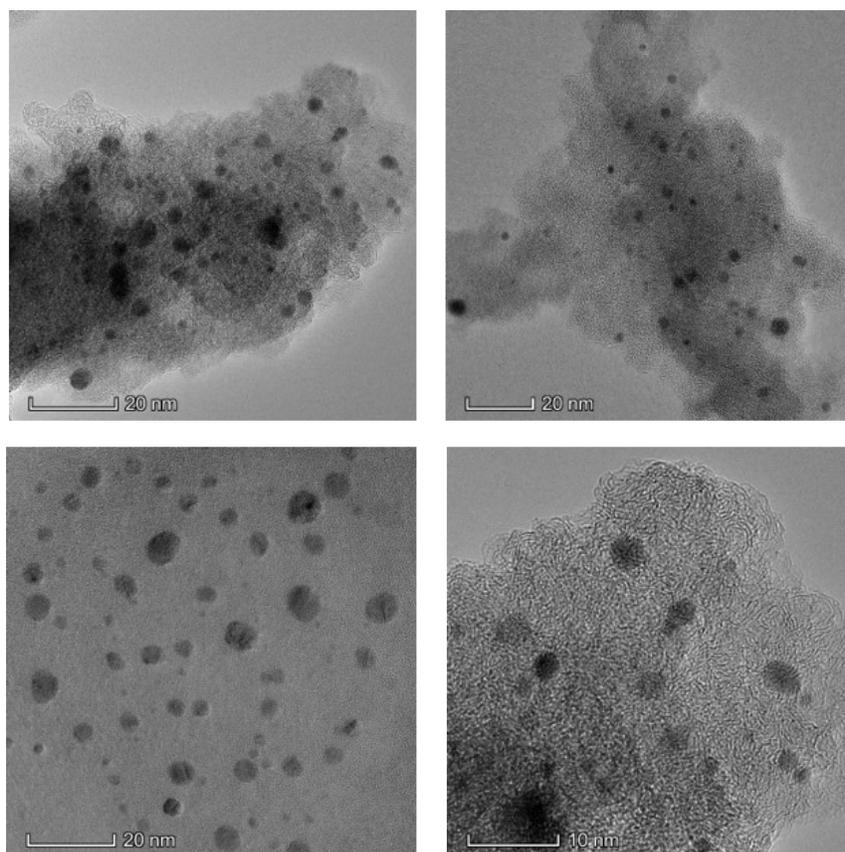
Figure S-6. HR-TEM images Ir/COF NP
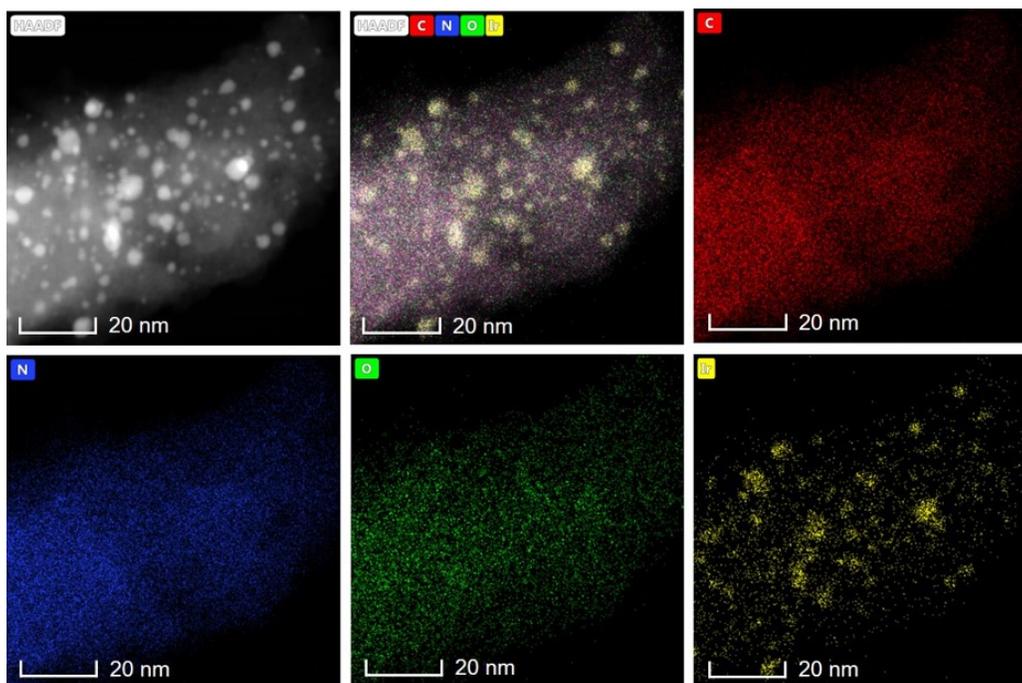
Figure S-7. HAADF-STEM Mapping images of Ir/COF NP
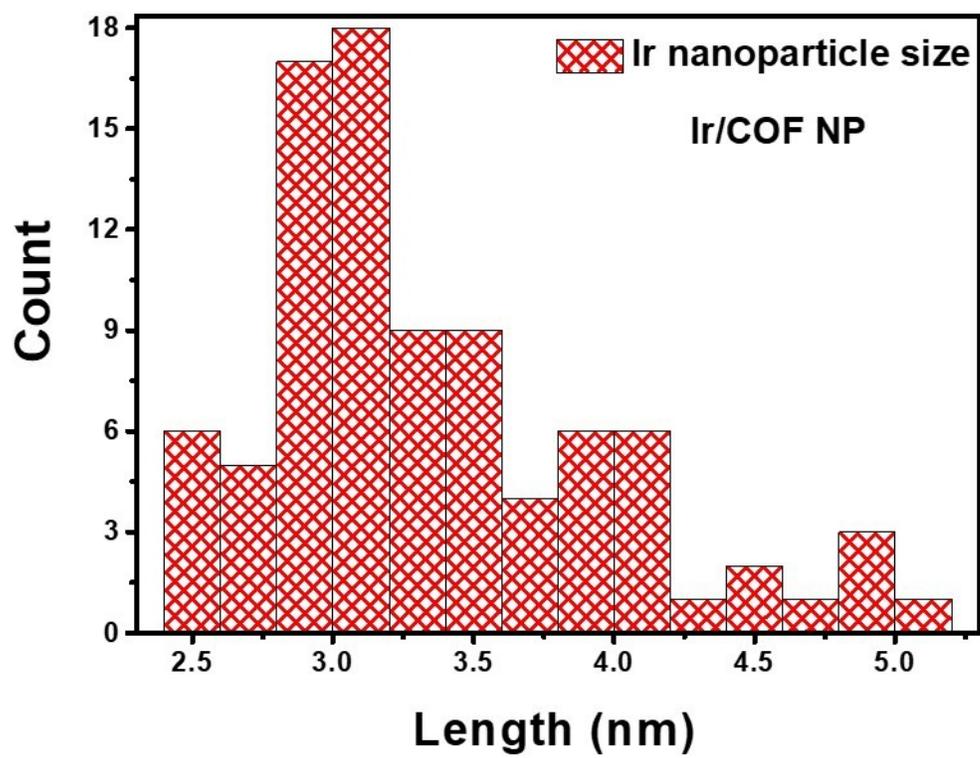
Figure S-8. Size distribution of Ir nanoparticles in the Ir/COF NP sample
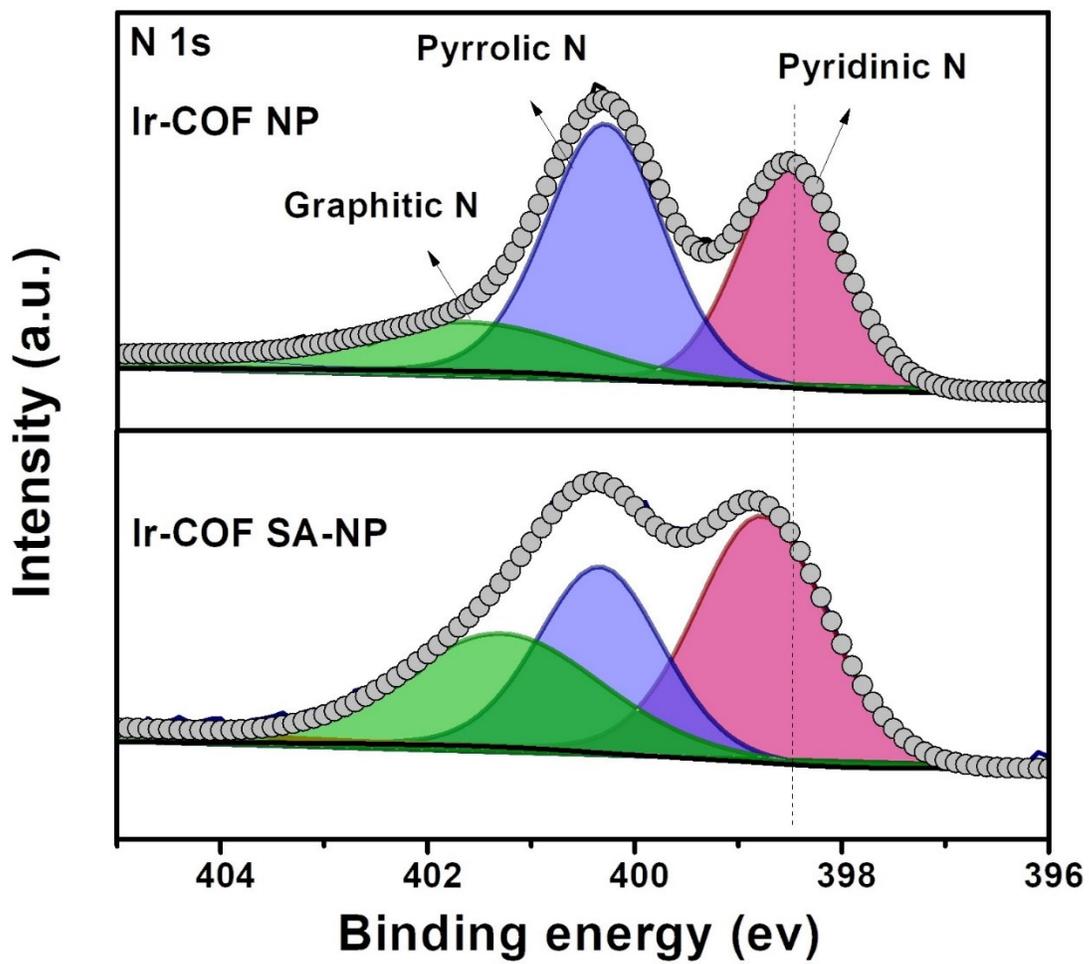
Figure S-9. N1s peak analysis of Ir/COF SA/NP and Ir/COF NP
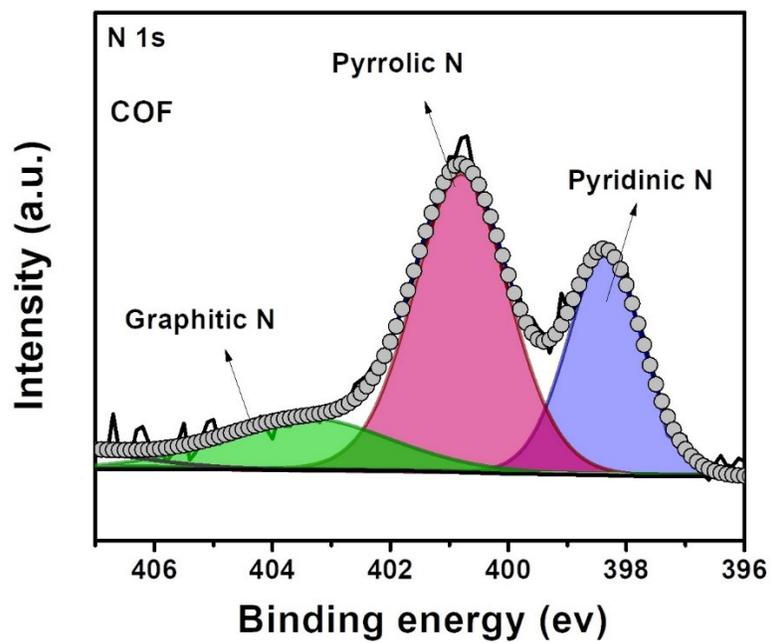
Figure S-10. N1s peak analysis of COF
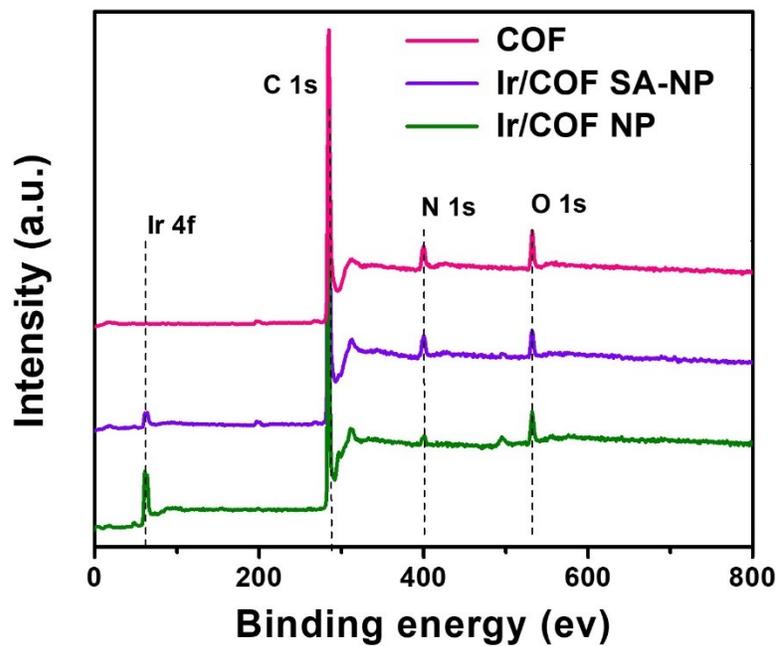
Figure S-11. XPS survey of Ir/COF SA/NP, Ir/COF NP and COF
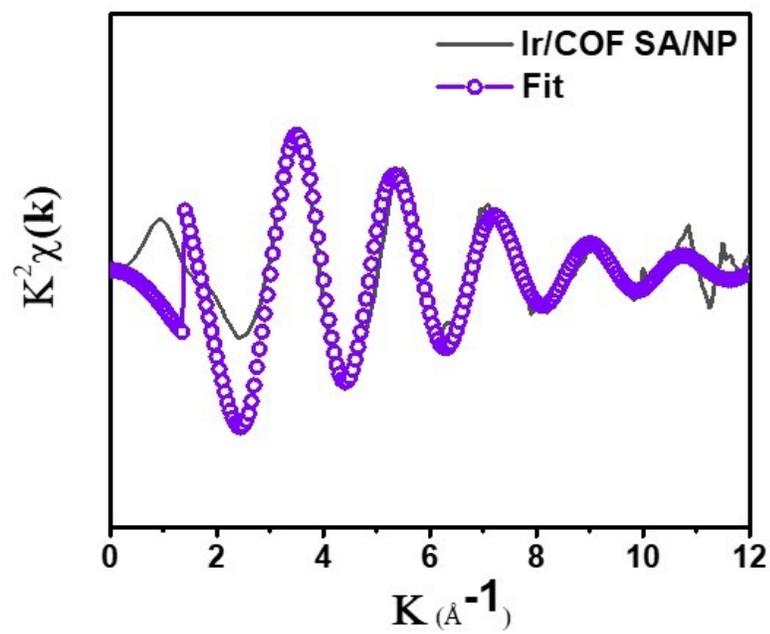
Figure S-12. EXAFS K-space fitting of Ir/COF SA/NP
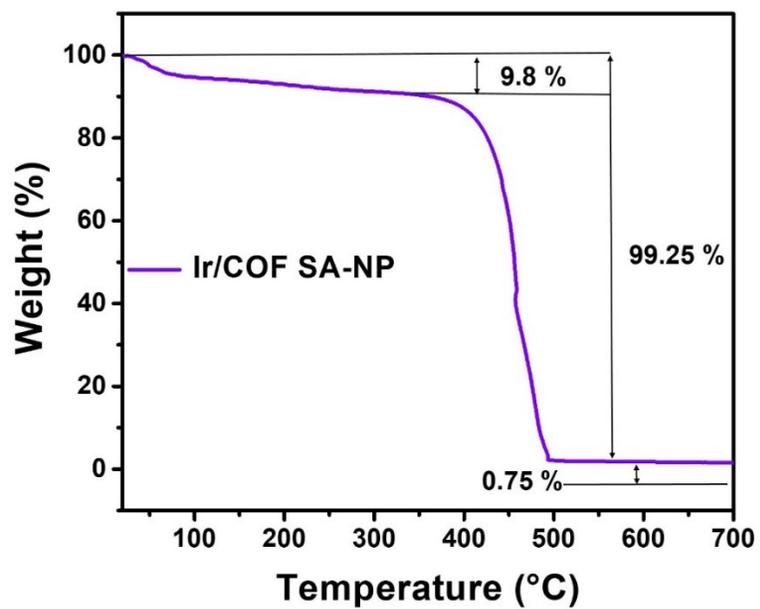
Figure S-13. TGA analysis of Ir/COF SA/NP
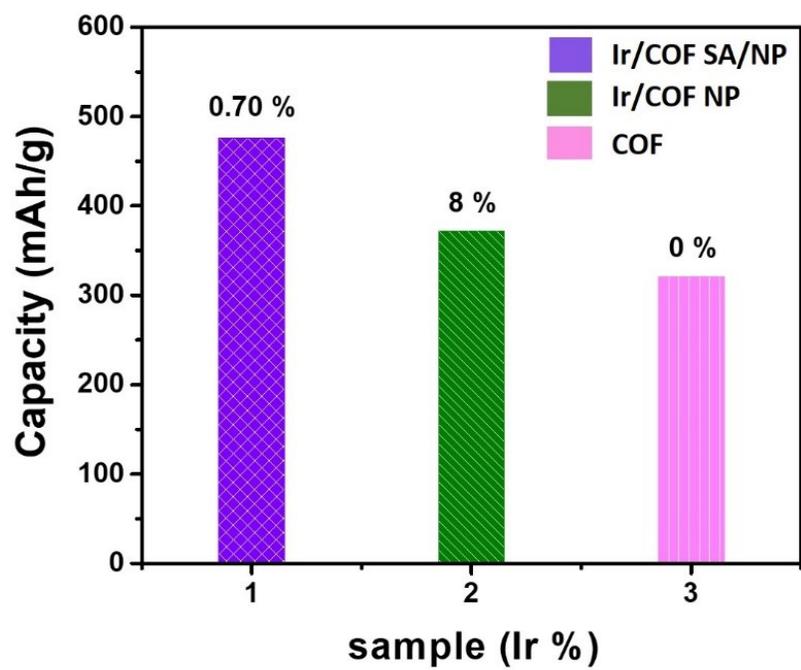
Figure S-14. Metal loading (Ir %) vs Specific capacity (mAh/g)
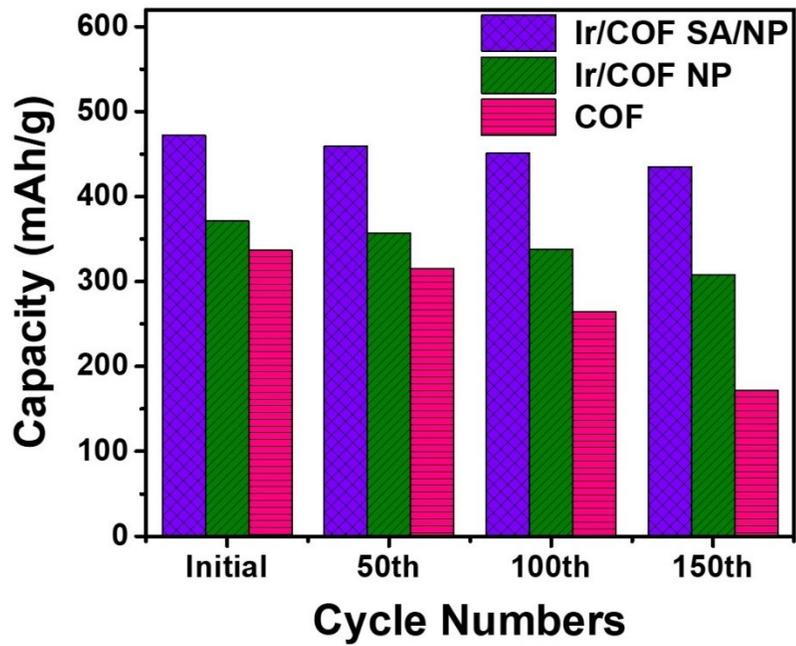
Figure S-15. Cycling performance
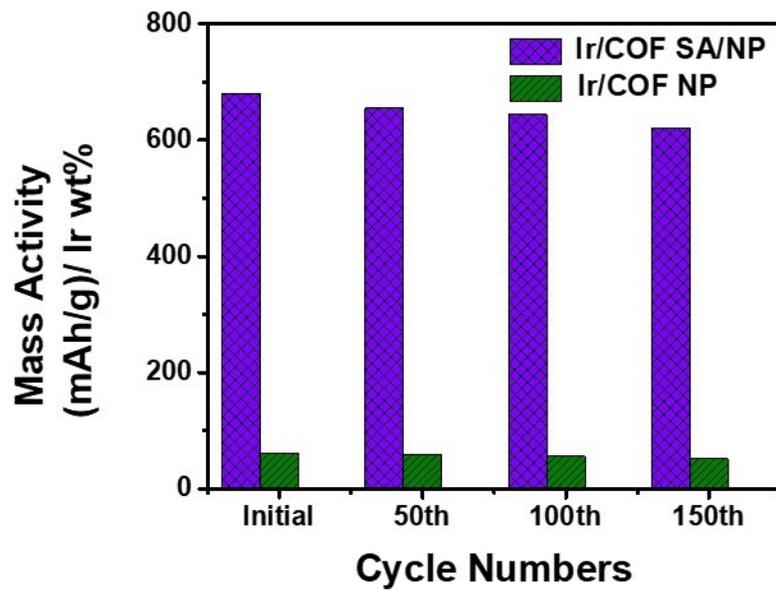
Figure S-16. Mass activity on the base of Ir% used in the cathode materials

Before cycling
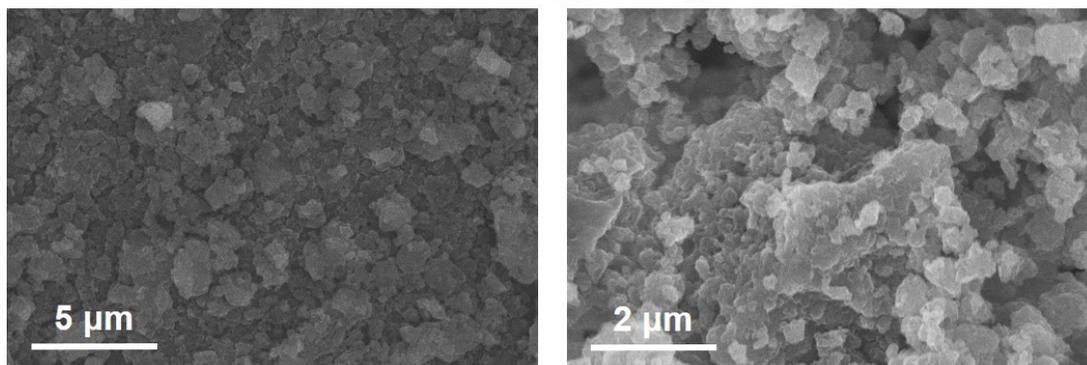
After 100 cycles
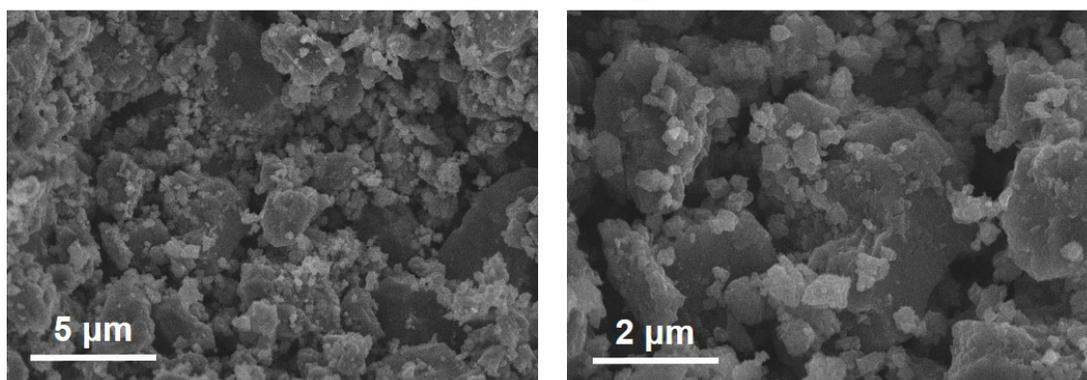
Figure S-17. SEM images of before cycling and after cycling of Ir/COF SA/NP cathode
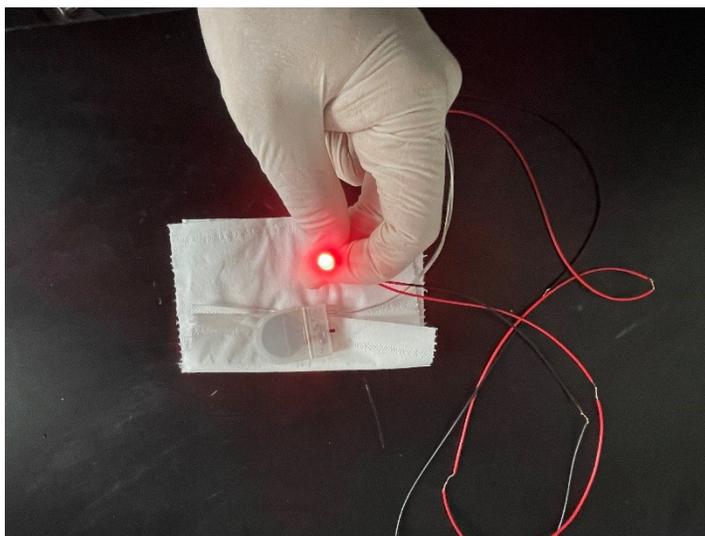
Figure S-18. LED test of the Ir/COF SA/NP based device at room temperature.

Sample	specific surface area	Pore volume	Pore size
COF	994.48 $m^2\,g^{-1}$	0.642 $cm^3\,g^{-1}$	3-15 nm
Ir/COF SA/NP	853.06 $m^2\,g^{-1}$	0.537 $cm^3\,g^{-1}$	3-15 nm
Ir/COF NP	762.94 $m^2\,g^{-1}$	0.520 $cm^3\,g^{-1}$	3-15 nm

Table S1. Brunauer-Emmett Teller (BET) analysis of Ir/COF SA/NP, Ir/COF NP and COF

Sample	Sell	CN	R (Å)	σ^2 (10^{-2} Å²)	ΔE_0 (eV)	r-factor (%)
Ir foil	Ir-Ir	12	2.70	0.2	6.1	0.6
Ir/COF SA/NP	Ir-N	5.4	2.12	0.7	7.3	0.4
	Ir-O	4	2.02	0.9	7.9	0.33

Table S2. The best-fitted EXAFS results of Ir/COF SA/NP.

[a]CN is the coordination number for the absorber-backscatterer pair, R is the average absorber-backscatterer distance, σ^2 is the Debye-Waller factor, and ΔE_0 is the inner potential correction. The accuracies of the above parameters are estimated as CN, ±20%; R, ±1%; σ^2, ± 20%; ΔE_0 , ±20%. The data range used for data fitting in k-space (Δk) and R-space (ΔR) are 3.0-11.4 Å^{-1} and 1.0-2.4 Å, respectively